JOURNAL OF APPLIED ELECTROCHEMISTRY 15 (1985) 685–696

The electrochemical behaviour of copper in alkaline solutions containing sodium sulphide

M. R. GENNERO DE CHIALVO, A. J. ARVIA

Instituto de Investigaciones Fisicoquímicas Teóricas y Aplicadas – INIFTA, Casilla de Correo 16, Surcursal 4, 1900 La Plata, Argentina

Received 11 September 1984

The electrochemical behaviour of copper in $NaHCO_3$ solution (pH 9) and NaOH solutions (pH 14) in the presence of sodium sulphide (10^{-3} to 5×10^{-2} M) was investigated by using rotating disc electrode and rotating ring-disc techniques, triangular potential scanning voltammetry and potentiostatic steps. When the potential increases from − 1.2 V upwards, copper sulphide layers are firstly formed at potentials close to the equilibrium potentials of the Cu/Cu_2S and Cu/CuS reversible electrodes. When the potential exceeds 0.0 V (NHE), the copper oxide layer is electroformed. Pitting corrosion of copper is observed at potentials greater than − 0.3 V. The charateristics of copper pitting are also determined through SEM optical microscopy and EDAX analysis. There are two main effects in the presence of sodium sulphide, namely, the delay in the cuprous oxide formation by the presence of the previously formed copper sulphide layer and the remarkable increase of copper electrodissolution when the potential exceeds the cuprous oxide electroformation threshold potential. These results are interpreted on the basis of a complex structured anodic sulphide layer and on a weakening of the metal–metal bond by the presence of adsorbed sulphur on the copper surface.

1. Introduction

Investigations on the electrochemical growth and structure of sulphide films on copper are relatively scarce despite their importance in many areas of applied chemistry and electrochemistry [1–4]. The growth of sulphide films on copper involves the formation of both stoichiometric and non-stoichiometric cuprous sulphides depending on the electroformation condition [5–9]. The anodic product can also be partly converted into cupric sulphide [10–12].

The presence of sulphur in the solution or in the metal itself enhances the dissolution of the metal and can possibly promote localized corrosion. This clearly occurs on sulphur covered nickel and nickel–iron alloys [14, 15]. This effect may be coupled with a delay in the formation of the passive oxide layer caused by the presence of the copper sulphide layer. The copper sulphide layer may also produce a localized corrosion of copper in the base electrode.

This paper attempts to elucidate some basic aspects related to the influence of sulphide ions in the electrochemical behaviour of copper in various alkaline electrolytes. The electrochemical and optical data show that the formation of an anodic complex copper sulphide layer precedes the anodic oxide film formation. The latter process is considerably influenced by the presence of the complex copper sulphide layer in two ways, namely by delaying the corresponding anodic process and by changing the cathodic potentiodynamic characteristics of the complex anodic copper oxide layer. Both effects are consistent with the formation of soluble copper species during the electrochemical process in the potential range of cuprous oxide formation, as postulated in the reaction mechanism recently discussed to interpret the latter reaction [16, 17].

2. Experimental procedure

The working electrodes were made from 99.9% copper either as wires (0.322 cm^2 apparent area) or discs (0.071 cm^2 apparent area) mounted in

0021-891X/85 $03.00 + .12

different PTFE holders. In any case the electrode surface was successively polished with different suspensions of alumina powder of decreasing grain from 1 μm down to 0.05 μm average diameter, and finally rinsed in triple distilled water. Before each run the electrode was cathodized at -1.2 V (vs Hg/HgO) for 3 min in order to start with a reproducible electroreduced surface. The working electrode was assembled in a three-compartment pyrex glass electrolysis cell and its potential was measured against a Hg/HgO/1 M NaOH reference electrode ($E^\circ = 0.100$ V) and corrected for the liquid junction potential. Potentials in the text are given in the NHE scale. The counterelectrode was a 4 cm^2 platinum sheet.

The electrolyte solutions covering the 8.5 to 14 pH range were prepared from AR $NaHCO_3$, Na_2CO_3, NaOH, $Na_2S \cdot 9H_2O$ and thrice distilled water. The additions of Na_2S were made to the nitrogen saturated base electrolyte covering the 10^{-3} to 5×10^{-2} M concentration range. Runs were made at $25 \pm 0.1^\circ$ C.

Potentiostatic polarization measurements were made by 0.05 V potential stepping and current reading after 5 min polarization at each potential step. The current transients under a constant potential step were also recorded. Conventional potentiodynamic current–potential profiles both under repetitive triangular potential sweeps (RTPS) and combined potential sweep-potential step perturbations were obtained. To establish the possible formation of soluble species during the voltammetric experiments a gold ring (0.035 cm^2 apparent area)-copper disc (0.125 cm^2 apparent area) rotating electrode was used. The collection efficiency was 0.25. The electrochemical measurements were complemented by SEM, optical observations and EDAX of the electrode surface.

3. Results

3.1. *Polarization curves*

The quasi-stationary potentiostatic current–potential (I/E) curves extending from -0.9 to 0.3 V range are strongly dependent on both the electrolyte composition and hydrodynamic conditions. For the quiescent 1 M $NaHCO_3$ solution (Fig. 1), a cathodic current appears below -0.7 V which is associated with molecular hydrogen

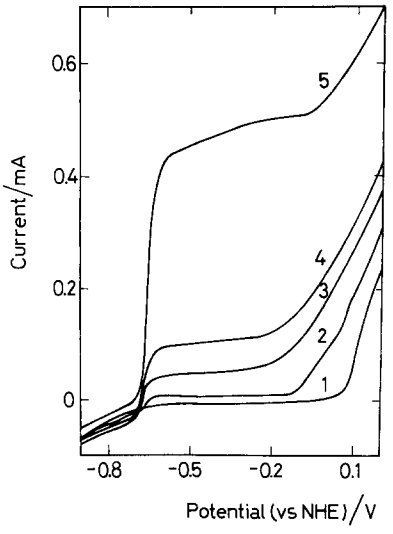

Fig. 1. Potentiostatic current–potential curves. Copper electrode in 1 M $NaHCO_3$ + x M Na_2S quiescent solution. (1) $x = 0$; (2) $x = 10^{-3}$ M; (3) $x = 5 \times 10^{-3}$ M; (4) $x = 10^{-2}$ M; (5) $x = 5 \times 10^{-2}$ M. Apparent copper electrode area 0.322 cm^2.

electroformation and an anodic current results at potentials greater than about 0 V which corresponds to cuprous oxide electroformation. When sodium sulphide is present in the electrolyte a clear transition from cathodic to anodic current occurs at about -0.7 V which is related to the formation of a copper sulphide film. The anodic limiting current observed in the -0.7 to -0.2 V range increases linearly with the concentration of sodium sulphide in solution (Fig. 2), although it is rather poorly defined at the largest sodium sulphide concentration.

The potentiostatic I/E curves run under rotation ($\omega = 200$ r.p.m.) in 1 M $NaHCO_3$ + 5×10^{-3} M

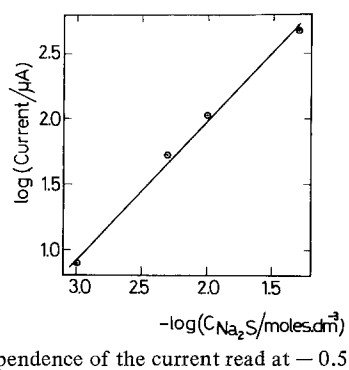

Fig.2. Dependence of the current read at -0.5 V on the Na_2S concentration in 1 M $NaHCO_3$. Quiescent solution (Data taken from Fig. 1).

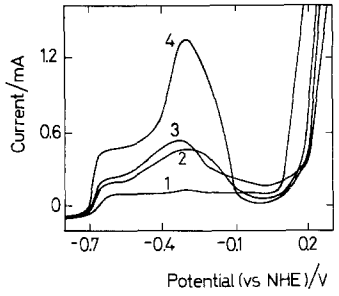

Fig. 3. Potentiostatic current–potential curves of copper electrode in 1 M $NaHCO_3$ + x M Na_2S under rotation (ω = 3000 r.p.m.). (1) $x = 10^{-3}$ M; (2) $x = 5 \times 10^{-3}$ M; (3) $x = 10^{-2}$ M; (4) $x = 5 \times 10^{-2}$ M. Apparent copper electrode area 0.125 cm^2.

Na_2S shows a limiting current nearly 2.5 times greater than that resulting with the stagnant solution. At $\omega > 800$ r.p.m. there is an initial limiting current extending up to about -0.5 V and an anodic current maximum. Under a constant rotation (ω = 3000 r.p.m.) the current read in the -0.65 to -0.5 V range (Fig. 3) increases linearly with the sodium sulphide concentration. In this case, the initiation of the oxide layer formation is shifted towards more positive values as the sodium sulphide concentration increases. Furthermore, a considerable increase of the anodic current at 0.1 V is noticed as both the sodium sulphide concentration and the stirring velocity are raised.

3.2. *Voltammetric runs*

A blank voltammogram run in 0.1 M $NaHCO_3$ + 0.1 M Na_2CO_3 (pH 9.80) at 0.2 V s^{-1} between -1.1 and 1.1 V (Fig. 4) shows the characteristic current peaks for electroformation (peaks I and II) and electroreduction (peaks III, IV, V and VI) of the complex copper oxide layer already described in the literature [16, 17]. The presence of sodium sulphide in the electrolyte (Fig. 5a–c) produces both anodic and cathodic additional peaks (peaks VII, IX and X), increases the current contributions from the base electrolyte and changes considerably the current peak distribution. As the sodium sulphide concentration increases the height ratio of current peaks I and II decreases and the cathodic current peak multiplicity corresponding to the electrochemical response of the system in the absence of sodium sulphide (Fig. 4) is no longer observed. On the other hand, the best definition of current peaks IX and X results at the lowest sodium sulphide concentration. The charge of both the anodic peak VII and the cathodic peak IX, is about 130 μC cm^{-2} (Fig. 5a). There is a relatively large potential difference between the voltammetric formation of copper sulphide and that of the copper oxide layer, as expected from equilibrium data [18].

The voltammogram run in the presence of sodium sulphide covering the -1.30 to -0.45 V range at 0.2 V s^{-1} changes during the first cycle (Fig. 6a) and after 30 min cycling two clear electroreduction current peaks are observed. These changes in the voltammetric response imply a constant cathode charge as well as a slight distortion and shift of the anodic peak towards more positive potentials.

The appearance of either a single or double anodic and cathodic peak depends on the anodic switching potential (E_a) value, on the sodium

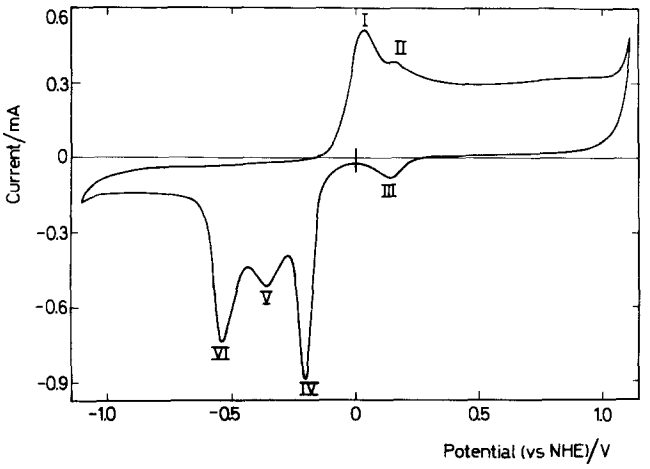

Fig. 4. Voltammogram run with copper electrodes in 0.1 M $NaHCO_3$ + 0.1 M Na_2CO_3 at v = 0.2 V s^{-1}. Apparent copper electrode area 0.322 cm^2.

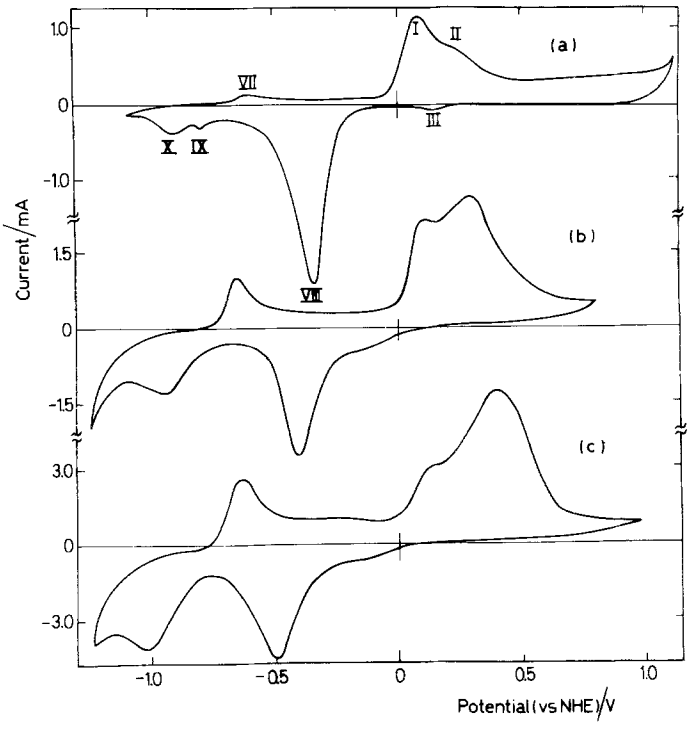

Fig. 5. Voltammograms run with copper electrodes in 0.1 M $NaHCO_3$ + 0.1 M Na_2CO_3 + x Na_2S at $v = 0.2\ V\ s^{-1}$. (a) $x = 10^{-3}$ M; (b) $x = 5 \times 10^{-3}$ M; (c) $x = 10^{-2}$ M. Apparent copper electrode area 0.322 cm^2.

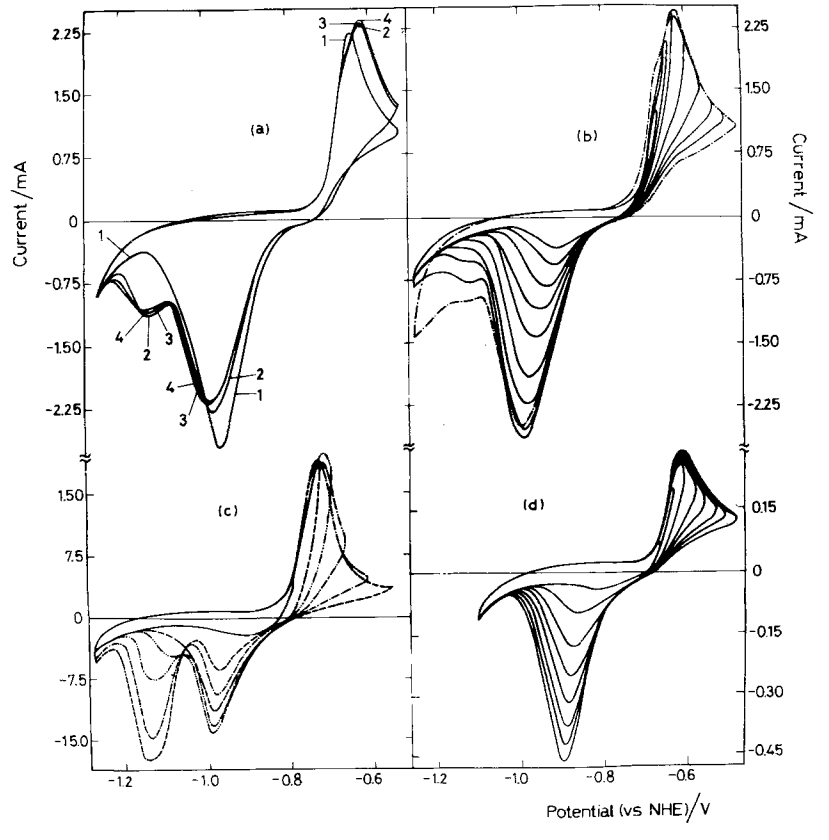

Fig. 6. Voltammograms run with copper electrodes in various electrolyte solutions + x M Na_2S at 0.2 $V\ s^{-1}$. Apparent copper electrode area 0.322 cm^2. (a) 0.1 M $NaHCO_3$ + 0.1 M Na_2CO_3 + 10^{-2} M Na_2S, (1) first TPS; (2) after 2 min RTPS; (3) after 10 min RTPS; (4) after 30 min RTPS. (b) 0.1 M $NaHCO_3$ + 0.1 M Na_2CO_3 + 10^{-2} M Na_2S. Influence of E_a. (c) 1 M NaOH + 10^{-2} M Na_2S. Influence of E_a. (d) 0.1 M $NaHCO_3$ + 0.1 M Na_2CO_3 + 10^{-3} M Na_2S. Influence of E_a.

sulphide concentration and on the solution pH (Fig. 6b–d). Thus, as either the sodium sulphide concentration or E_a are diminished a tendency to a stabilized voltammogram with a single pair of anodic and cathodic peaks is obtained. Conversely, double current peaks are systematically recorded at both large sodium sulphide concentration and pH and with E_a values more positive than -0.7 V.

The anodic current peak involves two contributions which are related to the two current peaks, one at about -0.97 V and another at -1.12 V (Fig. 6b). The cathodic peak multiplicity is enhanced as E_a becomes more positive. These results suggest that two different copper sulphide species are produced.

The height of peak VII increases linearly with the square root of v and its potential increases linearly with log v (Fig. 7a–b). Under comparable RTPS conditions the height of peak VII in the initial voltammogram changes linearly with the concentration of both sodium sulphide and OH^- ions in solution (Fig. 7c–d). The slope d log I/d pH is equal to 0.13. This slope is no longer observed during the following successive voltammograms probably due to the changes in the pH at the metal–solution interface, principally caused by the hydrogen evolution, which accompanies the electroreduction reaction of the anodic layer.

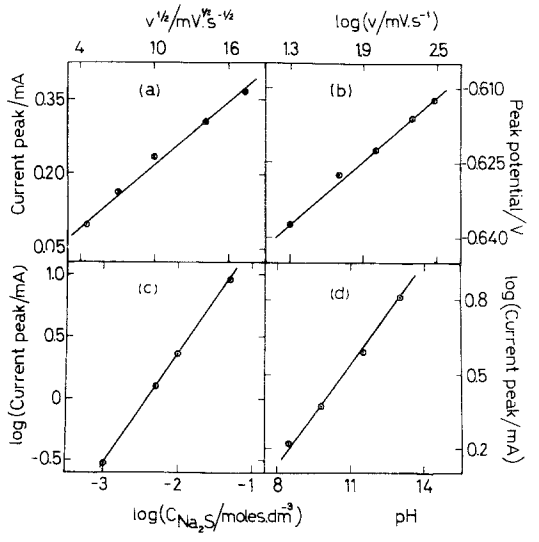

Fig. 7. (a) Dependence of height of current peak VII on $v^{1/2}$. (b) Dependence of the potential of current peak VII on log v. (c) Dependence of the height of current peak VII on sodium sulphide concentration. (d) Dependence of the height of current peak on pH. Apparent copper electrode area 0.322 cm^2.

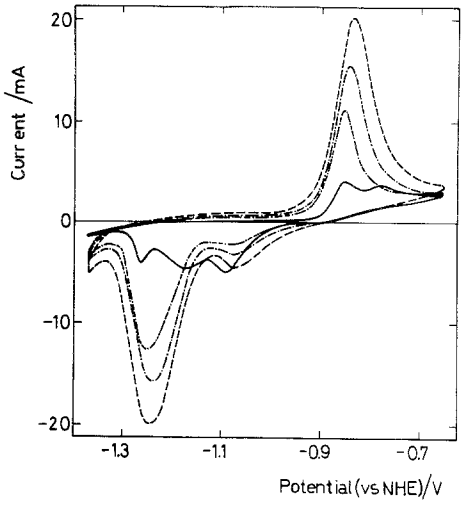

Fig. 8. Voltammograms run with copper electrodes in 1 M NaOH + 10^{-2} M Na_2S at 0.2 V s^{-1}. (——) first TPS; (— — · — — · — —) after 5 min RTPS; (— · — .) after 20 min RTPS; (— — — —) after 90 min RTPS. Apparent copper electrode area 0.322 cm^2.

At the largest sodium sulphide concentration, namely in 1 M NaOH + 10^{-2} M Na_2S, the voltammograms run between -1.25 and -0.55 V at 0.2 V s^{-1} show a considerable change during cycling together with a progressive increase in charge (Fig. 8). In this case, the first voltammogram resembles those reported in the literature [19] for electrochemical reactions involving non-stoichiometric copper sulphides.

The relative heights of peaks IX and X depend on the solution composition, but no appreciable changes in the potentials of peaks IX and X with the solution pH are noticed. The potential of peak X at about -1.0 V shifts linearly towards more negative values with log v. The charge ratio of these peaks and the equilibrium potential values of the Cu/Cu_2S ($E^\circ = -0.890$ V) and Cu/CuS ($E^\circ = -0.698$ V) electrodes suggest that for the same sodium sulphide concentration the formation of cupric sulphide at pH 14 is greater than at pH 9.

On the other hand, under rotation ($\omega >$ 2000 r.p.m.) the I/E curves exhibit a net current plateau (Fig. 9) extending from -0.7 to -0.6 V. The limiting current read at $E_a = -0.6$ V increases linearly with $\omega^{1/2}$ although the straight line does not intercept the origin of coordinates.

No soluble products were detected through the voltammetric runs made with the copper disc–gold ring rotating electrode. This result is in contrast

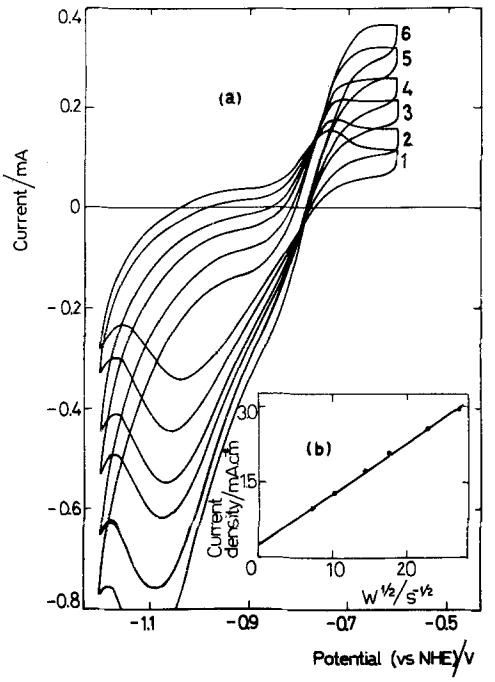

Fig. 9. (a) Voltammograms run with a rotating copper disc electrode in 0.1 M $NaHCO_3$ + 0.1 M Na_2CO_3 + 10^{-3} M Na_2S at 0.2 V s^{-1}. (1) 500 r.p.m.; (2) 1 000 r.p.m.; (3) 2 000 r.p.m.; (4) 3 000 r.p.m.; (5) 5 000 r.p.m.; (6) 7 000 r.p.m. (b) Plot of the apparent current density read at E_a vs $\omega^{1/2}$. Apparent copper electrode area 0.125 cm^2.

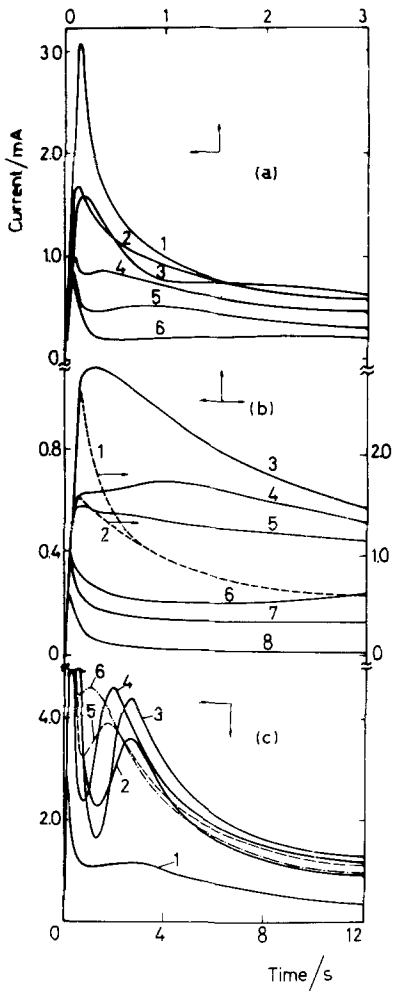

Fig. 10. Potentiostatic current transients at different E_s ($E_c = -1.2$ V). Apparent copper electrode area 0.322 cm^2. (a) 0.1 M NaOH + 10^{-2} Na_2S. (1) $E_s = -0.650$ V; (2) $E_s = -0.700$ V; (3) $E_s = -0.725$ V; (4) $E_s = -0.750$ V; (5) $E_s = -0.775$ V; (6) $E_s = -0.800$ V. (b) 1 M $NaHCO_3$ + 10^{-2} M Na_2S. (1) $E_s = -0.620$ V; (2) $E_s = -0.630$ V; (3) $E_s = -0.640$ V; (4) $E_s = -0.650$ V; (5) $E_s = -0.660$ V; (6) $E_s = -0.670$ V; (7) $E_s = -0.680$ V; (8) $E_s = -0.700$ V. (c) 1 M $NaHCO_3$ + 10^{-2} M Na_2S. (1) $E_s = 0.0$ V; (2) $E_s = 0.10$ V; (3) $E_s = 0.15$ V; (4) $E_s = 0.40$ V; (5) $E_s = 0.25$ V; (6) $E_s = 0.30$ V.

with previously reported data obtained by using the same experimental arrangement with NaOH solution in the absence of sodium sulphide [16].

3.3. *The open circuit potential*

The open circuit potential of copper in 1 M $NaHCO_3$ is -0.03 V and changes to -0.67 V when sodium sulphide is added to the base electrolyte in the 10^{-3} to 10^{-2} M range. The open circuit potential values remain constant for at least 12 h.

3.4. *The potentiostatic current transients*

Potentiostatic current transients in the potential range where the copper sulphide is formed ($-0.8 < E_s < -0.6$ V) were run by firstly stepping the potential to -1.20 V to avoid the spontaneous formation of a copper sulphide film, and later to E_s, where the anodic current transient was recorded (Fig. 10a and b). Under comparable conditions the current transients at pH 13 involve currents greater than at pH 8.5. At potentials lying in the range of peak VII, different contributions can be distinguished in the I/t records. At $E_s = -0.775$ V (Fig. 10a, curve 5), in the short time range ($t < 0.5$ s) the current transients fits a I vs $t^{-1/2}$ linear relationship. At the intermediate time range ($0.5 < t < 2$ s) a current maximum is observed. The latter increases in height and appears at shorter time as the potential step value increases. The current associated with pit growth increases

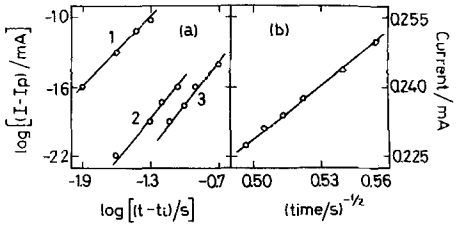

Fig. 11. Different plots of potentiostatic current transients, 0.1 M NaOH + 10^{-2} M Na_2S. (a) (1) $E_s = -0.725$ V; (2) $E_s = -0.750$ V; (3) $E_s = -0.775$ V. (b) $E_s = -0.775$ V.

with time according to the following relationship [20]:

$$I = I_p + K(t - t_i)^b \qquad (1)$$

where I is the current measured on the whole specimen area, I_p is the passivity current, t_i is an induction time and K and b are constants. The slope (b) of the log $(I - I_p)$ vs log $(t - t_i)$ plots is equal to 1.20 (Fig. 11a). The current decay ($E_s = -0.775$ V) observed in the long time range ($t > 2$ s) fits a I vs $t^{-1/2}$ relationship (Fig. 11b).

Current transients run by stepping the potential from -1.2 V to $0.0 < E_s < 0.3$ V, just in the potential range of copper oxide formation, are also complex as they involve the occurence of successive electrochemical reactions (Fig. 10c). In this case, however, the current increase after exceeding the minimum current also fits Equation 1 with $b \simeq 1.30$ (Fig. 12).

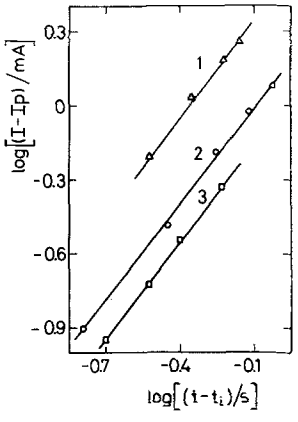

Fig. 12. Log $(I - I_p)$ vs log $(t - t_i)$ plot derived from the potentiostatic current transients. 1 M $NaHCO_3$ + 10^{-2} M Na_2S. (1) $E_s = 0.1$ V; (2) $E_s = 0.0$ V; (3) $E_s = 0.15$ V.

3.5. *Influence of copper sulphide on the copper oxide film formation*

Both voltammetric and quasi-stationary I/E curves show that when a copper sulphide film is formed the threshold potential for copper oxide electroformation shifts in the positive direction. Simultaneously a remarkable increase in the corresponding anodic and cathodic currents and a disappearance of the cathodic peak multiplicity is noticed. The increase in the anodic current is mainly associated with the contribution which has been already assigned to the formation of Cu(II) hydrous oxide species [16].

3.6. *Other physical and chemical data*

Optical and SEM microscopic observations of copper electrodes which have been potential cycled in the -1.2 to -0.5 V range, at 0.05 V s^{-1} during 1 h in 1 M $NaHCO_3$ + 10^{-2} M Na_2S, show the formation of a thick, dark granular layer of insoluble products, which after being removed, leaves the base metal surface with a large number of irregular shaped pits (Fig. 13a and b). The same result was obtained from a clean copper electrode which was firstly immersed into the solution, held at -1.2 V and stepped to E_s ($-0.6 < E_s < 0.3$ V) during 4 min (Fig. 14a and d). At $E_s = -0.6$ V, the optical observations already show the formation of a copper sulphide film. At a constant polarization time the number and the size of initial pits increase considerably when E_s is raised to the potential range of copper oxide formation. In this case, nearly spherical pits are formed and the pit base becomes apparently covered with a film which is more compact than the thick anodic film which extends over the rest of the metal. When the copper electrode is held at -0.6 V for 30 min in 1 M $NaHCO_3$ + 0.05 M Na_2S it becomes completely covered with a crystalline layer of anodic product (Fig. 15). Crystallographic characteristics [21] and EDAX results indicate that in this case the anodic layer corresponds to cupric sulphide. EDAX analysis of the anodic film formed at 0.2 V for 15 min in 1 M $NaHCO_3$ + 0.05 M Na_2S in the region outside the pit shows a Cu to S signal height ratio probably related to cupric sulphide, while the results from the pit base indicate the probable occurrence of either a

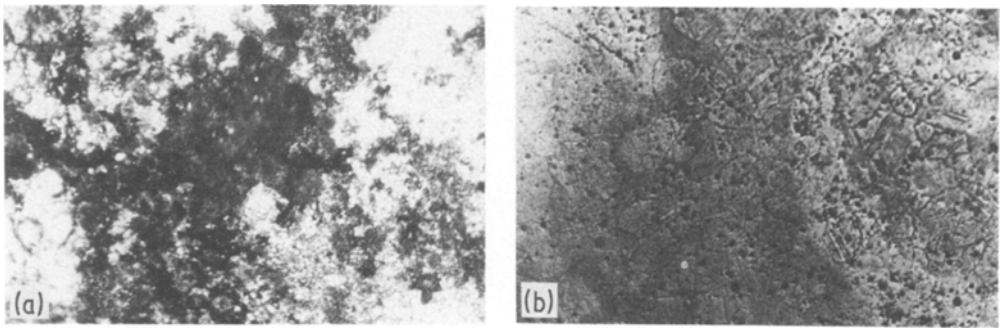

Fig. 13. (a) Microscopic observation (X 100) of a copper electrode which has been subjected to an hour RTPS between -1.2 and -0.4 V at 0.5 V s^{-1} in 1 M $NaHCO_3$ + 10^{-2} M Na_2S. (b) Microscopic observation (X 100) of the same electrode after removal of the anodic film by mechanical polishing.

cuprous sulphide or non-stoichiometric cuprous sulphide film within the pit (Fig. 16).

4. Interpretation and discussion

The equilibrium potentials at 25° C, for the electrochemical formation of Cu_2S and CuS are respectively [18]:

$$2\,Cu(s) + S^{2-}(aq) \rightleftarrows Cu_2S\,(s) + 2e\,;$$

$$E_1 = -0.890 + 0.0295\,p\,[S^{2-}] \qquad (2)$$

and

$$Cu\,(s) + S^{2-}(aq) \rightleftarrows CuS\,(s) + 2e$$

$$E_2 = -0.698 + 0.0295\,p\,[S^{2-}] \qquad (3)$$

In aqueous sodium sulphide solutions the concentration of ionic sulphur containing species are governed by the following pH dependent ionic equilibria [22]:

$$H_2S \rightleftarrows HS^- + H^+\,; \quad pK_4 = 7.04 \qquad (4)$$

and

$$HS^- \rightleftarrows S^{2-} + H^+\,; \quad pK_5 = 11.96 \qquad (5)$$

The electrochemical response of copper in the presence of sodium sulphide indicates that the anodic formation of the copper sulphide layer takes place in a potential range very close to the equilibrium potentials of the Cu/Cu_2S and Cu/CuS electrodes. This means that the potential is determined by the Cu/Cu (I) and Cu/Cu (II) in the presence of Cu_2S and CuS. The reactive species in solution can be related either to SH^- or to S^{2-} depending on the solution pH, according to the corresponding ionic equalibria 4 and 5. It should be noticed that the progressive addition of sodium sulphide to 0.1 M $NaHCO_3$ + 0.1 M Na_2CO_3 changes the solution pH from 9.88 to 10.37. Equilibria 2 to 5 are even more complex because of the participation of non-stoichiometric copper sulphides [5].

The electrochemical results, including the change in the open circuit potential value due to sodium sulphide addition can be related to the sulphidization of the copper surface [6]. In this case, thin films are composed mostly of Cu_2S [7]. The open circuit potential is very close to the equilibrium potential of Reaction 2. However, the complex voltammogram corresponding to the first stages of the reaction supports early interpretations that electrodeposited copper sulphide at low current density yields a layer of about 0.4 nm with a cubic structure probably related to $Cu_{1.8}S$ [5, 8, 13]. Therefore, it appears that the copper/sodium sulphide alkaline solution interface changes its structure during the reaction as follows:

Cu/electrolyte solution → $Cu/Cu_{1.8}S$/electrolyte solution → $Cu/Cu_{1.8}S/Cu_2S$/electrolyte solution → $Cu/Cu_{1.8}S/Cu_2S$/CuS/electrolyte solution.

Cu_2S is predominantly formed at potentials lower than -0.6 V while CuS is mainly produced at potentials more positive than -0.6 V. The accumulation of CuS is observed after a relatively prolonged electrolysis at a potential slightly exceeding that of Reaction 3. The final structure of the interface approaches that of a Cu_2S layer in direct contact with metallic copper covered by a secondary layer of CuS [7]. Therefore, the kinetics of the copper sulphide electroformation can be interpreted in terms of two successive stages. The

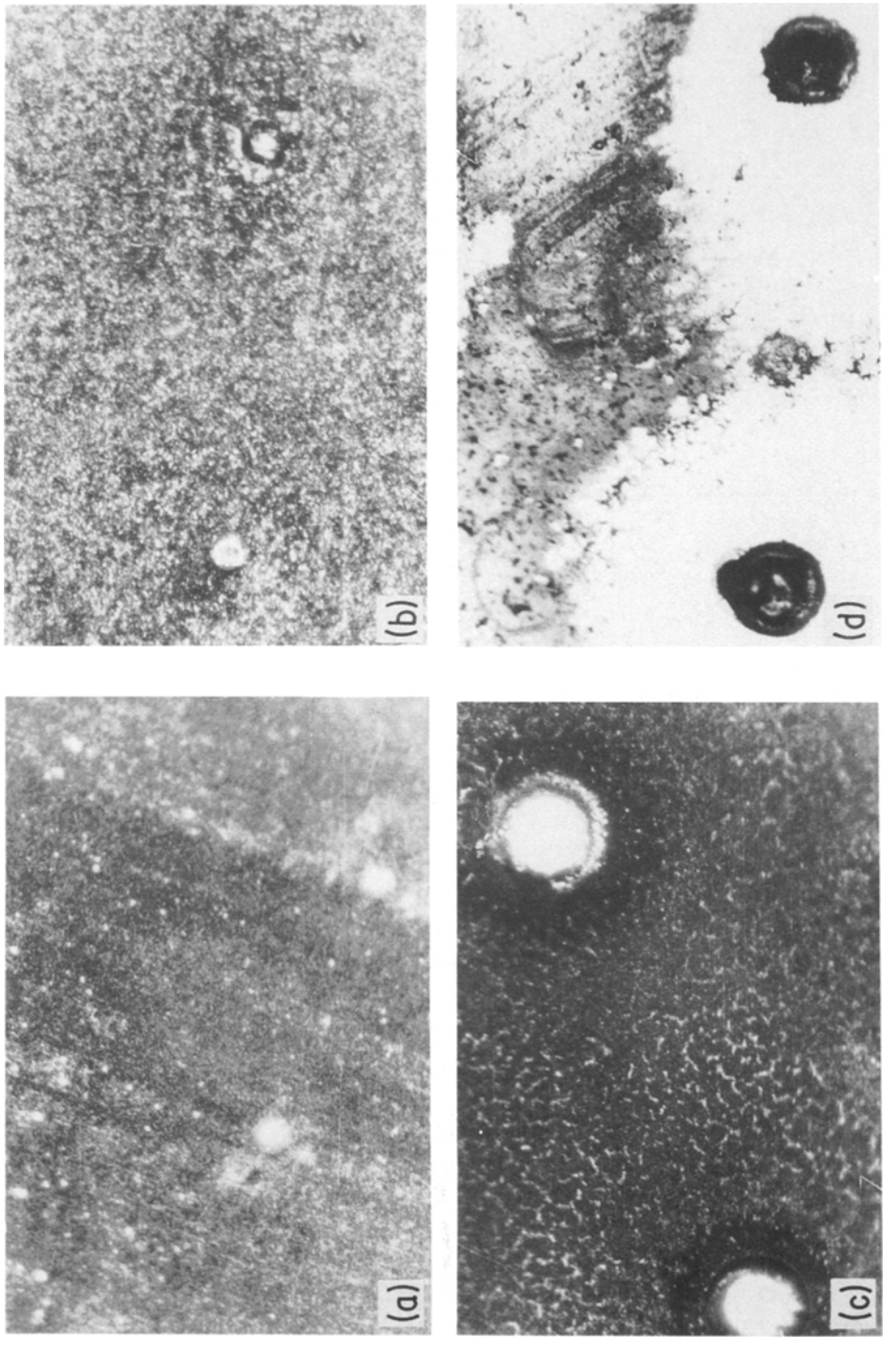

Fig. 14. Microscopic observation (× 100) of a copper electrode subjected to potentiostatic steps (4 min duration) from $E_c = -1.2$ V up to different E_s values in 1 M $NaHCO_3$ + 10^{-2} M Na_2S. (a) $E_s = -0.6$ V; (b) $E_s = -0.3$ V; (c) $E_s = 0.3$ V; (d) $E_s = 0.5$ V.

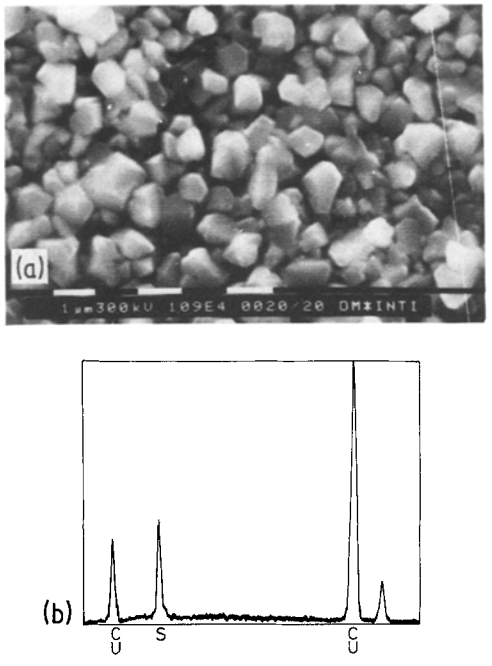

Fig. 15. (a) SEM pattern and (b) EDAX profile of the layer formed at -0.6 V during 30 min in 1 M $NaHCO_3$ + 5×10^{-2} M Na_2S.

first one, which corresponds to a relatively small charge, about $130\,\mu C\,cm^{-2}$, probably implies the formation of a single monolayer. The electroformation and electroreduction of this thin layer can be assigned to the voltammetric peaks observed in the -1.2 to -0.5 V range. These peaks are better defined at low sodium sulphide concentration. The corresponding reactions, which are formally equal to those related to Cu_2S electroformation, can be given in terms of anion electroadsorption/electrodesorption according to one of the following equations:

$$Cu + (HS^-)_i = Cu\,(HS)_{ad} + e \qquad (6)$$

or

$$2\,Cu + S^{2-} = (Cu_2S) + 2e \qquad (7)$$

depending on the ionic species prevailing at the solution pH at the interface, i. Both reactions give sulphur tightly bonded to the copper surface either in the form of an adsorbed $(HS)_{ad}$ layer or (Cu_2S) monolayer. The formation of the copper sulphide layer may proceed beyond the monolayer thickness, but in this case, the second level copper oxidation can occur yielding the cupric sulphide layer. The corresponding reactions are: either

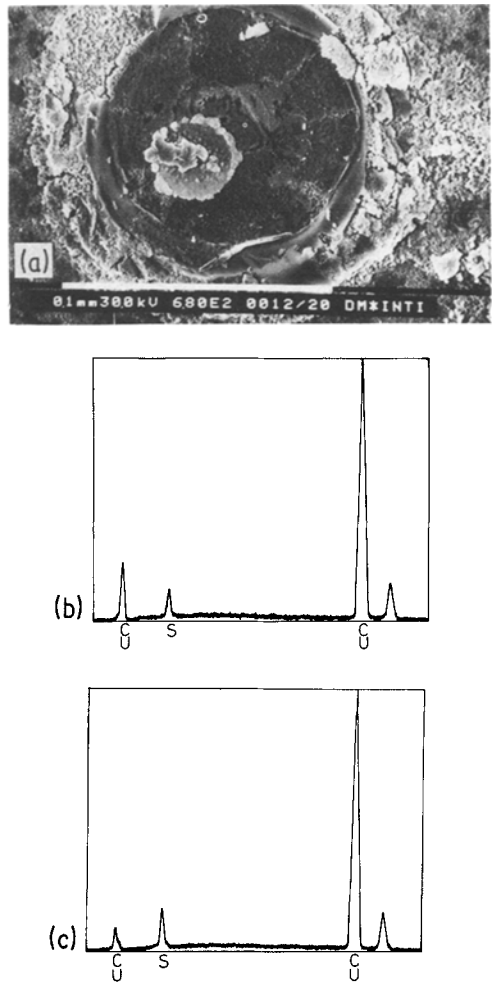

Fig. 16. (a) SEM pattern of the corrosion product obtained at 0.2 V during 15 min in 1 M $NaHCO_3$ + 10^{-2} M Na_2S. (b) EDAX profile of the outer layer. (c) EDAX profile of the inner layer.

$$Cu\,(HS) = CuS + H^+ + e \qquad (8)$$

or

$$Cu_2S + S^{2-} = 2\,CuS + 2e \qquad (9)$$

These reactions under steady state conditions either in the absence of stirring or under stirring become clearly mass transport controlled by the sulphide ion coming from the bulk solution to the electrode surface. The electrode surface becomes then covered by a thick layer of homogeneously crystalline cupric sulphide, as determined under potentiostatic conditions (Fig. 15). The formation of pits at potentials higher than 0.1 V is characterized by a cuprous sulphide film within the pit in

contrast with the thick cupric sulphide film outside the pit (Fig. 16). It seems likely that the localized copper electrodissolution is assisted by the presence of HS^- species which is the predominant one at pH 8–9 where the greatest localized attack of the base metal has been observed. In this case, the electrodissolution can be explained through a consecutive reaction pathway such as that recently found in localized corrosion of iron in sulphide-containing solutions [23]. In the case of copper this reaction pathway results:

$$Cu_n(Cu_2S)_{il}(z\ CuS)_{ol} + (HS^-)_i \rightleftarrows Cu_n(Cu_2S)_{il}(HS^-)_{ad}(z\ CuS)_{ol}; \quad (10)$$

$$Cu_n(Cu_2S)_{il}(HS^-)_{ad}(z\ CuS)_{ol} \rightleftarrows Cu_n(Cu_2S)_{il}(HS)_{ad}(z\ CuS)_{ol} + e; \quad (11)$$

$$Cu_n(Cu_2S)_{il}(HS)_{ad}(z\ CuS)_{ol} \rightleftarrows Cu_{n-1}(Cu_2S)_{il}[(z+1)\ CuS]_{ol} + (H^+)_i + e; \quad (12)$$

$$(H^+)_i + (S^{2-})_i \rightleftarrows (HS^-)_i \quad (13)$$

According to these reactions the localized attack initiates through the adsorption of HS^- ions in the interface at a pitting site covered by the inner compact Cu_2S thin layer (il). The adsorbed species participated into two electron transfer reactions yielding firstly $(HS)_{ad}$ intermediate and finally CuS which contributes to increase the thickness of the non-protecting CuS outer layer (ol). Reaction 12 contributes to the increase in the local acidification inside the pit [24] and to shift reaction [13] towards the right. The local formation of HS^- acts as a catalyst of the electrodissolution process.

When the potential reaches the range where the electroformation of copper oxides is expected, a delay of the electroformation of the copper oxide layer by the presence of the previously formed sulphide layer is observed. In the presence of sodium sulphide the latter reaction is appreciably inhibited while the copper sulphide layer covers the metal surface, but once the latter is broken, a remarkable increase in current is observed. This current increase is appreciably greater than that recorded in the absence of sodium sulphide (Figs 4 and 5). This current which is mainly associated with the formation of the copper oxide layer implies a strong localized corrosion of the base metal. The catalytic effect of the sulphur-containing species on the electrodissolution of copper can be explained through the accumulation of sulphur-containing species at surface defects above a certain critical coverage so that passivation by copper oxide species is no longer feasible and localized corrosion takes place there. In this case a non-protective sulphide layer is formed. In contrast, copper oxide formation will take place in those areas where the coverage by the copper sulphide species lies below the value of the critical coverage. This mechanism of localized corrosion of copper is to some extent similar to that already described for iron in sulphide-containing solutions and for nickel–sulphur corrosion in 0.1 M H_2SO_4 [14, 22]. It implies a weakening of the metal–metal bond by the presence of adsorbed sulphur on the metal surface. In this case, the potentiostatic current transients (Fig. 10) suggest that physical mechanisms of nucleation and growth are involved in the formation of both the copper sulphide layer and the copper pitting in the copper oxide electroformation potential range. The complete analysis of these transients under a wide range of experimental conditions permits a more detailed interpretation of the various film growth processes as well as copper pitting and is referred to in another publication [25].

Finally, voltammetric runs made in the presence of sulphide show the disappearance of the multiplicity of cathodic current peaks found under certain potential perturbation conditions for copper in alkaline solutions in the absence of sulphide ions because when the latter are present both Cu (I) and Cu (II) soluble species are removed from the solution at the interface as precipitated Cu_2S and CuS respectively. These results furnish an additional support to the mechanism of reaction earlier postulated for the kinetics of Cu_2O electroformation in base solutions, where the formation of soluble copper ions takes place during the anodic process. As these species are precipitated by sulphide ions the corresponding current peaks are no longer observed.

Acknowledgement

INIFTA is sponsored by the Universidad Nacional de La Plata, the Consejo Nacional de Investi-

gaciones Científicas y Técnicas and the Comisión de Investigaciones Científicas (Provincia de Buenos Aires). This work was also partially sponsored by the Regional Program for the Scientific and Technological Development of the Organization of American States.

References

[1] D. A. J. Rand, *J. Electroanal. Chem.* **83** (1977) 19.
[2] L. M. Peter, *Electrochim. Acta* **23** (1978) 1073.
[3] A. K. Covington, 'Ion Selective Electrodes', Vol. 1, CRC Press, Florida (1979).
[4] A. S. Baranski, W. R. Fawcett, A. C. McDonald, R. N. de Nobriga and J. R. McDonald, *J. Electrochem. Soc.* **128** (1981) 963.
[5] I. H. Usmani, *Phil. Mag.* **32** (1941) 89.
[6] T. P. Hoar and A. J. P. Tucker, *J. Inst. Metals* **81** (1952) 665.
[7] E. M. Khairy and N. A. Darwish, *Corr. Sci.* **13** (1973) 141, 149.
[8] M. Lamache and D. Bauer, *Anal. Chem.* **51** (1979) 1320.
[9] B. Scharifker, R. Rugeles and J. Mozota, *Electrochim. Acta* **29** (1984) 261.
[10] K. Fischbeck and O. Dorner, *Z. Anorg. Chem.* **182** (1929) 228.
[11] *Idem, ibid.* **184** (1929) 167.
[12] R. S. Bradley, *Trans. Faraday Soc.* **34** (1938) 278.
[13] B. C. Syrett, *Corrosion-NACE* **33** (1977) 257.
[14] J. Oudar and P. Marcus, *Appl. Surface Sci.* **3** (1979) 48.
[15] P. Marcus and J. Oudar, Proceedings on Fundamental Aspects of Corrosion Protection by Surface Modification, Vol. 84-3, The Electrochemical Society, edited by E. Mac Cafferty, C. R. Clayton and J. Oudar, (1984) p. 173.
[16] A. M. Castro Luna de Medina, S. L. Marchiano and A. J. Arvia, *J. Appl. Electrochem.* **8** (1978) 121.
[17] M. R. G. de Chialvo, S. L. Marchiano and A. J. Arvia, *ibid.* **14** (1984) 165.
[18] G. Milazzo and S. Coroli, 'Tables of Standard Electrode Potentials', J. Wiley, New York (1978).
[19] M. C. Brage, M. Lamache and D. Bauer, *Electrochim. Acta* **24** (1979) 25.
[20] J. Tousek, *Coll. Czech. Chem. Commun.* **37** (1972) 1454.
[21] S. Djurle, *Acta Chem. Scand.* **12** (1958) 1415.
[22] 'Handbook of Chemistry and Physics', (edited by R. C. Weast) 57th Ed, CRC Press, Florida (1976-77).
[23] R. C. Salvarezza, H. A. Videla and A. J. Arvia, *Corros. Sci.* **22** (1982) 815.
[24] J. R. Galvele, *J. Electrochem. Soc.* **123** (1976) 464.
[25] D. V. Vasquez Moll, M. R. G. de Chialvo, R. C. Salvarezza and A. J. Arvia, *Electrochim. Acta*, in press.